(NASA-CR-142859) INTERPLANETARY FIELD AND PLASMA DURING INITIAL PHASE OF GEOMAGNETIC STORMS (Denver Univ.) 31 p HC $3.75 CSCL 04A

N75-25360

Unclas

G3/46 22184

DEPARTMENT OF PHYSICS AND ASTRONOMY
DENVER RESEARCH INSTITUTE
UNIVERSITY OF DENVER

DENVER, COLORADO 80210

Technical Report DU-4963-7515

Interplanetary Field and Plasma During Initial Phase of Geomagnetic Storms*

V. L. Patel
M. J. Wiskerchen
Department of Physics and Astronomy
University of Denver
Denver, Colorado 80210

*Supported by National Aeronautics and Space Administration
Grant NGR-06-004-123

ABSTRACT

Twenty-three geomagnetic storm events during 1966-70 have been studied by using simultaneous interplanetary magnetic field and plasma parameters. Explorer 33 and 35 field and plasma data have been analyzed on large-scale (hourly) and small-scale (3 min.) during the time interval coincident with the initial phase of the geomagnetic storms. The solar-ecliptic B_z component turns southward at the end of the initial phase, thus triggering the main phase decrease in Dst geomagnetic field. When the B_z is already negative, its value becomes further negative. The B_y component also shows large fluctuations along with B_z. When there are no clear changes in the B_z component, the B_y shows abrupt changes at the main phase onset. On the small-scale behavior of the magnetic field and electric field ($\vec{E}=-\vec{V}\times\vec{B}$) studied in details for the three events, it is found that the field fluctuations in B_y, B_z and E_y and E_z are present in the initial phase. These fluctuations become larger just before the main phase of the storm begins. In the large-scale behavior field remains quiet because the small-scale variations are averaged out. The power spectrum analysis for few events using 5.11 data shows the steepening of the spectrum after the passage of the shock wave associated with the ssc. It appears that large as well as small time-scale fluctuations in the interplanetary field and plasma help to alter the internal electromagnetic state of the magnetosphere so that a ring current could start causing a geomagnetic storm decrease.

Introduction

Geomagnetic storms have been a subject of several early studies [Schmidt, 1917]. In recent years beginning with pioneering work of Chapman and Ferraro [1933] intense research studies have been carried out by the use of satellite borne experiments. Many features of the geomagnetic storm phenomenon are now understood [Akasofu, 1963; Gold, 1962; Parker, 1963; Piddington, 1963]. In particular, the presence of ring current in the magnetosphere has been proved to be the cause of the main phase decrease [Cahill, 1966; 1970]. The quantitative calculations and recent observations by Explorer 45 satellite [Cahill, 1973; Hoffman and Bracken, 1967; Smith and Hoffman, 1974] explain the main phase decrease in the geomagnetic field.

One aspect of the geomagnetic storm still remains unexplained; and that is the initial phase (IP). The IP is defined as the time-period of the magnetic fluctuations between the sudden commencement (ssc) and the main phase decrease. This time-interval may vary from 30 min to several hours. The physical conditions set-up during that time-interval are very important in that these conditions possibly determine whether the main phase will begin. It is known that the ssc's are caused by solar-originated shock waves or hydromagnetic discontinuities [Burlaga and Ogilvie, 1969]. Usually ssc's are associated with the geomagnetic storms but not all the storms have ssc's preceeding them [Akasofu, 1964]. During the initial phase of the storms, the solar wind pressure increases and the increase in the pressure is well correlated to the increase in the equatorial geomagnetic field represented by the Dst index [Virzariu, et al, 1972]. However, Akasofu (1964) has shown that this change in plasma pressure does not contribute to the main phase decrease of the storm. Because the magnitude of the ssc is not an indication if the storm will follow or not and the initial phase plasma pressure cannot show whether the storm will start, other factors need consideration.

Among other parameters, interplanetary magnetic and electric field, plasma temperature or composition of the plasma may play an important role in determining that the main phase decrease will follow the ssc in geomagnetic field. In general, there are indications that the geomagnetic activity represented by the indexes such as Ap or Kp is influenced by the interplanetary field [Patel et al, 1967; Schatten and Wilcox, 1967; Ballif et al, 1967 and Arnoldy, 1971]. However, these studies indicate only general nature of the phenomenon and study of individual events are considered by Hirshberg and Colburn [1969]; Patel and Desai, [1973]and Russell et al, [1974]. These studies were limited to a few events because of the limited availability of continuous interplanetary data. We have attempted to make comprehensive study of the large number of geomagnetic storms covering four years period between 1966 and 1970. During this four year interval good quality measurements of the interplanetary magnetic field and plasma were available from Explorer 33 and 35 satellites. Further, we have studied the interplanetary data on several time scales of the physical phenomena. The largest time scale used in the data analysis is one hour and the shortest time scale is 5.11 second. Many interesting features are discovered by the large scale (hourly) and small scale (minutes and seconds) field variations during the geomagnetic storms starting from ssc time to the onset of main phase of the storms. In several events, both magnetic field and plasma data were available and the study of the induced electric field $\vec{E} = -\vec{V} \times \vec{B}$ is carried out from small scale (minutes) to large scale (hourly) variations in the interplanetary space during the initial phase of the storms. The results obtained in this study involving geomagnetic storms confirm the conclusions derived from the limited number of events and reveal some new features showing large fluctuations which are discussed in later sections.

Data Selection

The identification of the geomagnetic storms included in this study was done by using numerical values and plots of the Dst index published by Sugiura and Poros (1971). We have set no restriction on the magnitude of the main phase decrease of the storm. However, the inclusion of the particular storm in this study was primarily decided on the availability of the simultaneous and continuous good quality interplanetary data. We have examined the magnetic field and plasma data from the Explorer 33 and 35 satellites for this study. In the final selection, during the period of August 1966 to November 1970, we had 23 magnetic storm events during which at least the magnetic field data on a large time scale (hourly) were available. Continuous field and plasma data were not available on all of these events for detailed analysis on a time scale of minutes. There are twenty events in which the interplanetary data were available with minor data gaps and these events were studied by using hourly averages of the interplanetary magnetic field. In the remaining three events, complete magnetic and plasma in the interplanetary space were available. We have carried out detailed study of these three events on a fine time scale of three minutes and five second averages. The interplanetary magnetic observations were studied in solar-ecliptic (SE) coordinates. Further, induced interplanetary electric field was studied in these three events by combining plasma velocity $\vec{V}$ and magnetic field $\vec{B}$ i.e. $\vec{E} = -\vec{V} \times \vec{B}$. Finally, power spectral analysis was carried out by using 5.11 second averages of the interplanetary magnetic field. Thus, the data analysis has been carried out on three different time scales, hourly, three minutes and 5.11 seconds. Details of the analysis in each case are described in appropriate place with the discussion in the text.

Large-Scale Interplanetary Magnetic Field During Initial Phase

In order to get some idea of the changes in the large-scale interplanetary magnetic field, we have analyzed twenty-three selected geomagnetic storms. Hourly averages have been calculated for the interplanetary field from the original data tapes containing 5.11 sec observations. We have exercised considerable care to exclude calibration points and some spurious data points in these hourly averages. As a rule, we felt that data points greater than 50 gammas rarely occur in the interplanetary space. The computer program will automatically reject such points. All hourly data points do not have equal number of 5.11 sec data points in them. We have demanded at least 30 min data in one hour averages. However, in the storm events we have studied, the interplanetary data in the initial phase of the storms had very good continuity in data collections. Whenever, data are sketchy and involve too many gaps, we have rejected that particular storm event.

For the selected twenty-three events, hourly values of solar ecliptic components B_x, B_y and B_z were plotted on the same time scale as the hourly Dst values. Out of these events, twenty storms had associated ssc or si. The remaining three events did not have identifiable ssc or si. We have used Dst values calculated by Sugiura and Poros [1971] and the ssc's were determined from a list published by IUGG reports. Because the data analysis involves large amount of the interplanetary as well as ground geomagnetic data, it is not possible to publish every event on diagrams. We will summarize the most important features of the events and discuss later on three events in detail. In these three events, continuous data of magnetic field and plasma were available on three minute time scale. We have been able to study hourly large-scale changes as well as small-scale variations on a three minute scale and 5.11 sec scale in these events.

We have given the details of twenty-three geomagnetic storms and the interplanetary magnetic field in Table 1. Because a very large amount of information has been condensed in this table, some explanation is necessary. The main phase onset (T_i) is determined from the Dst values when the continued decrease begins in Dst value for several hours. The plots of Dst prepared by Sugiura and Poros (1971) are used as a guide. The average value of Dst at T_i UT hours is taken as base value (B_i) for the standard base in calculating the main phase decrease of the storm. This value of B_i is within 5 gammas from the average of a few hours steady Dst value before the main decrease starts. Finally, the maximum decrease in the storm is determined from the Dst values as B_{max} occuring at UT time T_{max}. The difference between B_{max} and B_i determines the maximum decrease of the storms. We note that the events we have studied have storm decrease of 235 gammas to the smallest one having 30 gammas. The small decreases actually are small storm events accompanied by the events with decreases of 68 to 117 gammas (e.g., storms of Nov. 6, 7, 1970, Sept, 6, 7, 1968 and December 13, 14, 1966).

The length of the initial phase is determined by using the onset of the main phase (T_i) and occurrence time of ssc. The difference between these two UT times is the initial phase (ΔT_i) of the storm. These ssc times are accurate within a few minutes but the subjectivity in the determination of the T_i makes error of $\pm$ 1 hour. The ssc times have been rounded to the closest hour because Dst values are hourly values. Within these conditions the length of the initial phase for the storm is anywhere from one hour to 13 hours. This analysis compares well with the study made by Antsilevich[1967]. Other parameters of interest are time required to complete the continued decrease and the rate of decrease in the storm. The time (ΔTmp) is defined as the difference between T_{max} where the maximum decrease is registered and the time of onset of the main phase T_i. The value of Δ Tmp for the storm events in the Table is from 3 to 32 hours. The smaller value of Δ Tmp means that the main phase decrease is completed faster compared to the storms that have large values. We have also calculated the rate of decrease for the storm events listed in the Table. The rate is obtained from the maximum decrease ΔB and the time Δ Tmp required to effect the decrease. The ratio $\Delta B/\Delta Tmp$ has a range of 1.9 to 33.6 gammas/hour. The highest rate of decrease occurs in the biggest storm (March 23, 1969) and the lowest rate of decrease is evident in one of the smallest storms on March 5, 1970. Apparently, the storm events studied in this paper do not show any consistent relationship between the rate of decrease and the magnitude ΔB of the storm.

The large-scale interplanetary magnetic field during the initial phase of twenty-three storms has been analyzed by studying hourly values of B_x, B_y and B_z solar-ecliptic components. Primarily, the component B_y and B_z are considered because they are important in ..luencing electromagnetic state of the magnetosphere through internal convection patterns and the reconnection processes. These processes have been described in details in a review paper [Nishida, 1975]. The component B_x signifies the sector boundaries of the interplanetary field and sector-boundary effect is not considered in this study.

In the Table, we have given the ranges of fluctuations of the B_y and B_z components during the initial phase. The limits indicated in the Table are the upper and lower limit of the fluctuations, e.g., the storm on February 16, 1967 has interplanetary field component B_y which fluctuates between -20 to +7 gammas and B_z fluctuates between 2 to 13 gammas remaining positive during the initial phase. When an average value of B_y or B_z is listed in the Table, the field has been more or less steady with that given value of B_y or B_z. The magnitude of the storm decrease is not related to the fluctuating or quiet large-scale magnetic field during the initial phase. Some of the large storms, March 8, 1970 ($\Delta B = 114\ \gamma$) have highly varying B_y and B_z components with the variations as large as 27 gammas. Some other storms having large main phase decreases ($\Delta B = 117\gamma$ on Nov. 7, 1970 and $\Delta B = 110\ \gamma$ on Feb. 7, 1967) have steady and quiet B_y and B_z components.

The most conspicuous behavior of the interplanetary field occurs at the end of the initial phase. The B_z component at the onset time of the main phase (end of initial phase) turns southward (negative) from the northward (positive) in 16 storm events out of 23 events studied. Whenever the B_z is already southward before the main phase begins, its negative value further becomes more negative in four storm events. In twenty storm events (out of 23 events studied), the change in the B_z component seems to be an important parameter (within $\pm$ 1) in causing the onset of the main phase. In the remaining three events (2/28/68; 9/7/68 and 5/14/69), no abrupt change in B_z component is observed. As far as the B_y component is concerned, we have not observed as consistent behavior as the B_z component. The B_y component has shown some large variations that might incldue the change of the direction or merely change in magnitude. When B_z does not show clear change, correspondingly B_y also does not show variations in these storms. Some factors other than interplanetary field becomes important in starting the main phase .

Small-Scale Interplanetary Fields During Initial Phase

It has been possible to study twenty-three geomagnetic storms using hourly averages of the interplanetary data. However, it has been possible to study only these events on the small-scale by using 3 min averages of the magnetic and plasma data. We have selected 3 min time period only because the plasma data were available on that time scale. Detailed study has been carried out for these three storms using magnetic field solar ecliptic components B_x, B_y and B_z and the plasma parameters: density (per cc), bulk speed and plasma flow directions in terms of ecliptic longitude and latitudes. The three minute average of magnetic field was formed by using original data points of 5.11 sec from the data tapes. Usual caution was exercised to eliminate calibration and spurious points. Further, electric field components were calculated by matching 3 min solar wind plasma velocity and interplanetary field. In calculating electric field $\vec{E} = -\vec{V} \times \vec{B}$, the values of $\vec{E}$ were omitted in computer program when gaps in V or B existed.

We discuss important features of the small-scale variations in the interplanetary field and plasma for these three storms during initial phase. First, data on the Feb. 7, 1967 event are shown in Fig. 1. There are two ssc's observed in this event. One at 1416 UT (eleven observatories)and another at 1636 UT (50 observatories). In the first ssc the solar wind data show a small rise in plasma density. The solar wind speed is not considerably changed but note the marked change in solar wind plasma flow longitudinal direction. Such large changes exceeding 10° are rare in plasma directions. However, the second ssc at 1636 UT seems to be the major cause of the disturbances. The plasma velocity changes from 450 to 650 km/s and the density rises from 5 to 20 particles/cc. The flow direction in latitude shows larger than 10° fluctuations. Correspondingly, the magnetic field components

B_x, B_y and B_z all show fluctuations of 10 to 15 gammas. Such fluctuations are not seen on the large scale variation in hourly averages (Table 1). When electric field component E_x, E_y and E_z are calculated and plotted in Fig. 1, only E_y and E_z components show large variations of $\pm$ 15 mV/m. Further, the variations were examined for the electric field by computing $\Delta E = E_i - E_{i-1}$ where E_i is the ith point in 3 min averages time series. It is very clearly shown in Fig. 1, that the electric field fluctuations begin with the second ssc. The ssc at 1636 UT is the main cause of the large fluctuations in the interplanetary fields. The fluctuations in E_y and E_z (corresponding to B_y and B_z) are predominent in the initial phase, while E_x has no significant perturbations. The large perturbations diminish when the main phase proceeds to show decrease in the hourly Dst. The storm decrease observed on the earth is about 110 gammas.

Another storm of the same magnitude occurred on Feb. 15-16, 1967 during which detailed interplanetary data were available. There are two ssc's in this event: 2348 UT on Feb. 15 and 0835 UT on Feb. 16. In the Table, we have considered 0835 UT ssc as the beginning of initial phase because it is the nearest time to the onset of the main phase decrease. However, the interplanetary data and the rise in the geomagnetic field indicate that the initial phase begins at 2348 UT on Feb. 15, as shown in Fig. 2. The first ssc appears to have been caused by a shock-wave which is apparent (Fig. 2) in solar wind plasma data. The plasma density rises from 10 to 25 per cc and the plasma velocity from 300 to 450 km/s. The most remarkable is the change in the plasma flow angle of latitude exceeding 10°. The interplanetary field which was very quiet before the arrival of the shock-wave begins to fluctuate in B_y and B_z components within $\pm$ 15 gammas. Similar fluctuations are best seen in ΔE_z and ΔE_y plots in Fig. 2. Note that the extremely quiet E_y and E_z field component show large fluctuations as shown in ΔE_y and ΔE_z coincident with the ssc. The fields have very quiet configuration before ssc. The electric field fluctuations include variations in both B and V and the plasma flow angles. The geomagnetic storm is apparently triggered by the second ssc at 0833 UT on Feb. 16. This ssc does not have very large changes in velocity, but the density decreases from 15 to 5 per cc. It is possible that the second ssc is related to reverse shock wave in the interplanetary space. The magnetic and electric field changes are very large as seen in Fig. 2. The B_z component quickly changes to negative value (-15γ) from the positive value of 15γ. The B_y component simultaneously changes from negative to positive value. The fluctuations are reflected in E_y and E_z electric field components in which 15 to 20 mV/m fields are observed before the main phase of the storm starts. These field values are the largest fluctuations observed in the initial phase of the geomagnetic storms. The variations ΔE_y and ΔE_z in Fig. 2 also show larger fluctuations associated with the second ssc.

In Fig. 3 is shown the interplanetary condition in the storm of Feb. 10, 1968. The ssc on the ground is seen at 1621 UT. The interplanetary plasma data show a shock wave indicated by the rise in the plasma density and velocity. The field and plasma conditions are extremely quiet before the ssc. The fluctuations in the field components of $\vec{E}$ and $\vec{B}$ field are shown in the initial phase. The main phase decrease begins with B_z component making a chnage from positive to negative value, while B_y also changes from positive to negative value. The initial phase time duration is also characterized by the fluctuations in E_y and E_z and the ΔE_y and ΔE_z. The interplanetary field and plasma fluctuations are smaller than the Feb. 15-16, 1967 event.

In order to study simultaneous variations in Y and Z components of the interplanetary field, we have combined E_y and E_z and plotted them vectorially as shown in Fig. 4. Because $\vec{E}$ is calculated from $-\vec{V} \times \vec{B}$ and $\vec{V}$ is mostly radial i.e., $V \approx V_x$, the $+B_y$ corresponds to $+E_z$ and $-B_z$ corresponds to $+E_y$. As stated previously in the vector representation YZ solar-ecliptic plane, near the onset of the main phase of the storms E_y turns positive ($-B_z$) and E_z (B_y) is positive or negative (e.g., Feb. 15-16, 1967 event). The details of the simultaneous variations in E_y and E_z are shown in Fig. 4 for the three storm events.

For a limited amount of continuously available data, power spectrum analysis was carried out by using 5.11 sec data. Dynamic power spectra were obtained for a two hour period of time for B_x, B_y, B_z and XY and XZ plane projections near the ssc associated shock wave. Three such events were studied in which continuous good data at 5.11 sec interval were available. The Fast Fourier Transofrm computer algorithm based on work of Cooley and Tukey [1965] was used. The Cooley-Tukey algorithm restricts the number of points to 2^n where n is integer. We have selected 256 points of data at 5.11 sec intervals. The power spectra were obtained by using first 256 points, then again calculated for 256 points segment starting at 128th point. Thus overlapping of 128 points is continued until two hour interval is completed. The origianl 5.11 s data points were examined for calibration and bad data points. The rejected or missing data points were filled by linear extrapolation. If the gap exceeded 8 data points, a linear detrending was applied to 256 point interval. The power spectra from 5.11 sec data are presented in Figs. 5, 6 and 7. The data are analyzed around ssc at 2348 UT on Feb. 15, 1967; 0835 UT on Feb. 16, 1967 and 1621 UT on Feb. 10, 1968.

Two distinct slopes are apparent in frequency range 10^{-3} to 10^{-2}Hz and 10^{-2} to 10^{-1} Hz in Figs. 5, 6 and 7. The dashed curves in these figures represent several sample power law dependencies on frequency if the power $P(f) \propto f^{-\beta}$. Previous studies estimate $\beta = 1$ to 1.5 for quiet conditions and $\beta = 1.5$ to 3 for disturbed conditions [Sari and Ness, 1969]. The important observation in Figs. 5, 6 and 7 is that the spectrum is steepened after the shock. The pre-shock β values are $1.0 \leq \beta \leq 1.5$ while post-shock values are $2.0 \leq \beta \leq 3.0$. The change in power law near and after the shock is apparent in the center diagram (2338-2400 UT) in Fig. 5, the fourth diagram (0819-0841 UT) in Fig. 6 and the center diagram (1600-1621 UT) in Fig. 7. These intervals are the interplanetary shock phenomena (slightly different time from the earth observed ssc UT times). The change in spectral slope is larger in Y and Z components as compared to X component. One would expect this result because the Y and Z components show larger variations in original data. The spectral energy is larger in Y and Z components than that in X components. The result of analysis of the XY and YZ projection is not shown in diagrams because it does not contain any more information than that represented in Y and Z components power spectrum analysis.

Summary and Discussion

The study of the initial phase of 23 geomagnetic storms with simultaneous interplanetary fields and plasma indicates that in most of these events, the solar-ecliptic Z component (B_z) of the interplanetary magnetic field turns southward when the main phase decrease begins [Hirshberg and Colburn, 1969; Patel and Desai, 1973; Russell et al., 1974]. Further, it is noted that if the field has negative B_z component in the initial phase, then it becomes more negative when the main phase decrease starts (see Table 1). When both of these statements do not hold for the B_z component, the B_y component reversal (positive to negative or vice-a-versa) or the sharp change in magnitude occurs. Only two events (5/14/69; 9/7/68) did not show any significant change near the main phase onset but exhibited large fluctuations in B_z or B_y during initial phase. The change in B_z component is similar to that found in five storm events in 1968 by Russell et al., and the Feb. 15-16, 1967 storm studied by Hirshberg and Colburn [1969]. However, in our extensive study of the 23 storm events, we find that large variations of B_y are also found with those appearing in B_z. When the B_z variations are not so pronounced in some storm events, B_y variations seem to play the important role in initiating the main phase decreases of the storm. The variations in B_y and B_z are observed on the large-scale (hourly) and small-scale (3 min) fluctuations of the fields in the interplanetary space. Another important observation of the small-scale fluctuations shows that the initial phase is marked with the irregular (possibly hydromagnetic turbulence) fluctuations in the interplanetary space as shown in Figs. 1 to 4. Both magnetic field components B_y and B_z and the electric field components E_y and E_z (in three events studied) show especially large fluctuations just before the main phase onset time. The small-scale electromagnetic fluctuations are best seen in ΔE_y and ΔE_z. Such small-scale fluctuations are averaged out in the data containing hourly averages and therefore are not apparent in large-scale observations. Power spectrum analysis carried out for a few selected events also indicates that the spectrum is steepened in the initial phase near and after the shock. The low frequency fluctuations in 10^{-3} to 10^{-2} Hz have larger power contents.

In physical terms, the initial phase of the storms contain large-scale (hourly) as well as small-scale (3min to 5.11 sec) fluctuations. These interplanetary field fluctuations somehow help to change the electromagnetic conditions in the magnetosphere so that the ring current particles mainly protons of 1 to 1000 kev energy could enter the magnetosphere. The southward B_z which appears in almost all the storms when the main-phase decrease starts, help to make connection between the interplanetary and magnetosphere fields as suggested by Dungey [1961]. The reconnection regionsin the sunward side and the tail region are possible locations where the solar plasma can enter the magnetosphere. The fluctuations in the B_y component could alter the plasma convection patterns in the magnetosphere Nishida, [1975]. The fluctuations in the interplanetary space exhibited in ΔE_y and ΔE_z and the corresponding variations in the magnetosphere could possibly accelerate the particles to ring current energies so that the main phase decrease could proceed. The definitive acceleration mechanisms are unknown at this time.

This study indicates that large as well as small-scale fluctuations in the initial phase of the storm are always present and become enhanced before the main phase starts. However, many questions remain unanswered. For example, what determines the length of the intial phase and why certain main phase decreases have large or small magnitude under almost similar interplanetary conditions. In general, it is found that large geomagnetic storm decreases are associated with large fluctuations in the interplanetary space during the initial phase. However, there are events in which the interplanetary field and plasma show very large changes and the geomagnetic storm has only moderate decrease in the Dst [Hoffman et al, 1974]. Further study of many events on the large and small time-scale using simultaneous observations in the interplanetary space, magnetosphere and geomagnetic data are needed to find answers to these unsolved problems of the geomagnetic storm.

ACKNOWLEDGEMENTS: We thank John A. Van Allen and Dr. A. Goldman for very valuable advice in computer programming related to the computer plots and power spectrum analysis. The interplanetary data (Magnetic Data: Dr. N. F. Ness and colleagues; Plasma Data: MIT group) were obtained from National Space Science Data Center, Greenbelt. We thank J. King, D. Hei and L. Davis for their prompt help in data acquisition. The major portion of the computer work was carried out at the National Center for Atmospheric Research, Boulder Computer Facility which is operated by the National Science Foundation. This research has been supported by the National Aeronautics and Space Administration-Grant NGR-06-004-123.

References

Akasofu, S. I., The main phase of the magnetic storms and the ring current, Space Sci. Rev., 2, 91, 1963.

Akasofu, S. I., A source of the energy for geomagnetic storms and auroras, Planet. Space Sci., 12, 801, 1964.

Antsilevich, M. G., Duration of the initial phase of a geomagnetic storm, Geom. and Aeron., 7, 265, 1967.

Arnoldy, R. L., Signature in the interplanetary medium for substorms, J. Geophys. Res., 76, 5189, 1971.

Ballif, J. R., D. E. Jones, P. J. Coleman, L. Davis, Jr. and E. J. Smith, Transverse fluctuations in the interplanetary magnetic field, a requisite for geomagnetic variability, J. Geophys. Res. 72, 4357, 1967.

Burlaga, L. F. and K. Ogilvie, Causes of sudden commencements and sudden impulses, J. Geophys. Res., 74, 2815, 1969.

Cahill, L. J., Inflation of the inner magnetosphere during a magnetic storm, J. Geophys. Res., 71, 4505, 1966.

Cahill, L. J. Magnetosphere inflation during four magnetic storms in 1965, J. Geophys. Res., 75, 3778, 1970.

Cahill, L. J. Magnetic storm inflation in the evening sector, J. Geophys. Res. 78, 4724, 1973.

Chapman, S., and V. C. A. Ferraro, A new theory of geomagnetic storms, Terrest. Magn. Atmosph. Elect., 38, 79, 1933.

Cooley, J. W., and J. W. Tuckey, An algorith for the machine calculation of complex Fourier series, Math. Comput., 19, 297, 1965.

Dungey, J. W. Interplanetary magnetic field and the auroral zones, Phys. Rev. Letters, 6, 47, 1961.

Gold, T., Magnetic Storms, Space Sci., Rev., 1, 100, 1962.

Hirshberg, J. and D. S. Colburn, Interplanetary field and geomagnetic variations - A unified view, Planet. Space Sci., 17, 1183, 1969.

Hoffman, R. A. and P. A. Bracken, Higher order ring currents and particles energy storage in the magnetosphere, J. Geophys. Res. 72, 6039, 1967.

Hoffman, R. A., L. J. Cahill, R. R. Anderson, N. C. Maynard, P. H. Smith, T. A. Fritz, D. J. Williams, A. Konaradi, and D. A. Gurnett, Explorer 45 observations of the magnetosphere and magnetopause during the August, 4-5, 1972 magnetic storm period, Goddard Space Flight Center, Report Z 621-74-114, 1974.

Nishida, A., Interplanetary field effect on the magnetosphere, Space Sci. Rev., 17, 353, 1975.

Parker, E. N., Dynamics of the geomagnetic storms, Space Sci. Rev., 1, 62, 1962.

Patel, V. L., Cahill, L. J. and A. J. Dessler, Magnetosheath field geomagnetic index Ap and stability of the magnetospause, J. Geophys. Res. 72, 426, 1967.

Patel, V. L. and U. D. Desai, Interplanetary magnetic field and geomagnetic D_{st} variations, Astrophys. and Space Sci., 20, 431, 1973.

Piddington, J. H., Theories of the geomagnetic storm main phase, Planet Space Sci., 11, 1277, 1963.

Russell, C. T., R. L. McPherron, and R. K. Burton, On the causes of the geomagnetic storms, J. Geophys. Res., 79, 1105, 1974.

Sari, J. W., and N. F. Ness, Power spectra of the interplanetary field, Solar Phys., 8, 155, 1969.

Schatten, K. H. and J. M. Wilcox, Response of the geomagnetic activity, index Kp to the interplanetary magnetic field, J. Geophys. Res. 72, 5185, 1967.

Schmidt, A., Erdmagnetismus Enzyklopadie Enzyklopadie der mathematischen Wissenschaften, Band VI, B. 10, 265, Leipzig. 1917.

Smith, P. H. and R. A. Hoffman, Direct observations in the dusk hours of the characteristics of the storm time ring current particles during the beginning of magnetic storms. J. Geophys. Res. 79, 966, 1974.

Sugiura, M. and D. J. Poros, Hourly values of equatorial D_{st} for the years 1957-1970, Goddard Space Flight Center Report X-645-71-278, 1971.

Verzariu, P., M. Sugiura and I. B. Strong, Geomagnetic field variations caused by changes in quiet -time solar wind pressure, Planet, Space Sci., 20, 1909, 1972.

Figure Captions

Fig. 1 February 7, 1967 storm event with equatorial Dst index and Explorer 33 magnetic field solar ecliptic components B_x, B_y and B_z. The field components are 3 min averages. Plasma data show change in bulk speed V, number density (particles/cc) and plasma flow angles. The electric field components shown are obtained by $\vec{E} = - \vec{V} \times \vec{B}$. The change in the electric field (ΔE) components show large fluctuations in the initial phase of the storm.

Fig. 2 February 15-16, 1967 storm event. The data shown are from Explorer 33 with the description given in Fig. 1. Note unusually large fluctuations in the plasma flow direction during the initial phase of the storm.

Fig. 3 February 10, 1968 storm event. Explorer 33 interplanetary data are similar to that described in Fig. 1. Note the fluctuations in plasma flow directions and electric field components.

Fig. 4 Electric field components in solar-ecliptic coordinates calculated from interplanetary magnetic field and solar wind plasma are projected into yz plane to show simultaneous variation of y and z components for the storm events on Feb. 7, Feb. 15-16, 1967 and Feb. 10, 1968.

Fig. 5 Power spectra calculated from 5.11 sec Explorer 33 magnetic field data in interplanetary space for storm event of Feb. 15-16, 1967. X, Y, Z are designated for solar-ecliptic components B_x, B_y and B_z. Note the spectral change with passage of a shock wave (center figure). Data time interval used in the analysis is shown at the top of each of the figures. Sample power-dependence is illustrated by the dotted lines.

Fig. 6 Power spectra calculated from Explorer 33 5.11 sec interplanetary data for B_x, B_y and B_z components. Note spectral changes during 0819 - 1841 UT (third block) when second shock corresponds to the second ssc on Feb. 16, 1967.

Fig. 7 Power spectra calculated from Explorer 33 5.11 sec interplanetary magnetic field data. Note the spectral changes at and after the shock (beginning with center block) during Feb. 10, 1968 storm event.

Table Caption

Table 1. Interplanetary magnetic field variations in the initial phase of the geomagnetic storms. For each storm event: T_i is the time when the main phase decrease begins, B_i is the Dst value at T_i, Bmax and Tmax are the Dst value and the time when the storm decrease is maximum. ΔT_i is the time length of initial phase, ΔB is the magnitude of the storm decrease, ΔTmp the time required to complete the decrease i.e. $(T_{max}-T_i)$, the rate of decrease $\Delta B/\Delta$Tmp and the interplanetary field variations in the initial phase and at the beginning of the main phase (end of the initial phase). The ssc-UT is the time observed at the earth.

TABLE 1

		Main Phase				Initial Phase	Main Phase			Interplanetary Field In Initial Phase Maximum Variations		Change in Interplanetary Field at Main Phase**	
Date	SSC-UT	T_i	B_i	B_{max}	T_{max}	ΔT_i	ΔB	ΔT_{mp} (hours)	$\frac{\Delta B}{\Delta T_{mp}}$	B_y (gammas)	B_z (gammas)	B_y (gammas)	B_z (gammas)
8/29/66	1315	2000	25	- 67	0300 8/30	0700	92	0700	13.1	~-5	±2	- 1 to + 3	+ 4 to -10
8/30/66	1112	1700	15	-110	2400	0600	125	0700	17.9	~-10	- 2 to +10	- 7 to -13	+ 8 to -15
10/ 4/66	1314	2000	45	- 70	0400 10/5	0700	115	0800	14.4	-12 to + 5	+ 2 to + 8	+ 5 to -20	+ 7 to -15
12/13/66	0109	0400	22	- 31	1900	0300	51	1500	3.4	+ 2 to - 7	+ 3 to - 2	+ 1 to +17	- 2 to -10
12/14/66	1225	1400	-10	- 95	2000	0200	85	0600	14.2	~+15	0 to + 2	+15 to 0	0 to -18
2/ 7/67	1636	1800	11	-121	2400	0200	110	0600	18.3	~-7	~ 8	- 7 to -15	+ 8 to - 8
2/16/67	0835	1000	- 6	-120	1400	0200	114	0400	28.5	-20 to + 7	+ 2 to +13	-20 to + 6	+12 to -17
5/ 2/67	1012 1030	1900	- 4	-130	0500 5/3	0900	126	1000	12.6	~ 10	- 2 to +10	0 to -15	-15 to -20
12/30/67	1006	2300	- 9	-106	2300 12/31	1300	97	2400	4.0	~ 10	±3	~ 10	- 2 to -17
2/10/68	1621	1800	-17	-123	0800 2/11	0200	106	1400	7.6	~-2	0 to + 2	- 2 to -12	+ 2 to -12
2/27/68	None	1900	1	- 37	0200 2/28		38	0700	5.4			- 4 to - 8	+ 3 to - 8
2/28/68	None	1300	- 7	- 75	2300		68	1000	6.8			- 5 to -17	-8
9/ 6/68	1488 1823*	2100	11	- 28	2400	0600 0300	37	0300	12.3	~-7	- 2 to + 8	no change(-)	+ 5 to - 5
9/ 7/68	1047* 1409*	2000	- 7	- 95	0800 9/8	1000 0600	88	1200	7.3	~-12	0 to -10	no change(-)	no change(-)
2/10/69	2024	2200	- 9	- 63	0200 2/11	0200	54	0400	13.5	~+3	+2	+ 3 to - 7	+ 2 to -10
2/11/69	0739+	1000	-57	-121	2000	0200	64	1000	6.4	~ 4	-10	+ 4 to - 3	-10 to - 2
3/19/69	1441 1958	2300	- 5	- 64	0300 3/20	0800 0300	59	0400	14.8	~+2	~ 4	+ 2 to -9	+ 3 to - 5
3/23/69	1012 1826	1900	- 5	-240	0200 3/24	0900 0100	235	0700	33.6	- 2 to -12	+ 4 to - 6	-12 to + 2	+ 3 to -18
5/14/69	1929	2200	- 6	-133	0500 5/15	0300	127	0700	18.1	0 to -15	0 to + 3	no change(-)	no change(+)
3/ 5/70	0805	1800	10	- 51	0200 3/7	1000	61	3200	1.9	-12 to + 4	+ 2 to +10	no change	+ 2 to - 5
3/8/70	1417	1800	-46	-268	2300	0400	222	0700	31.9	-13 to 0	- 6 to +16	0 to +25	+16 to -15
11/ 6/70	None	0300	- 2	- 29	1100		31	0800	3.9			+ 8 to - 3	0 to - 7
11/ 7/70	0046	0200	15	-102	1000	0100	117	0800	14.6	~+12	~+3	+13 to +18	+ 3 to - 7

** When Main Phase starts within ±1 hour

* SI Checked by 68 observatories

\+ minor SSC at two observatories

ORIGINAL PAGE IS
OF POOR QUALITY

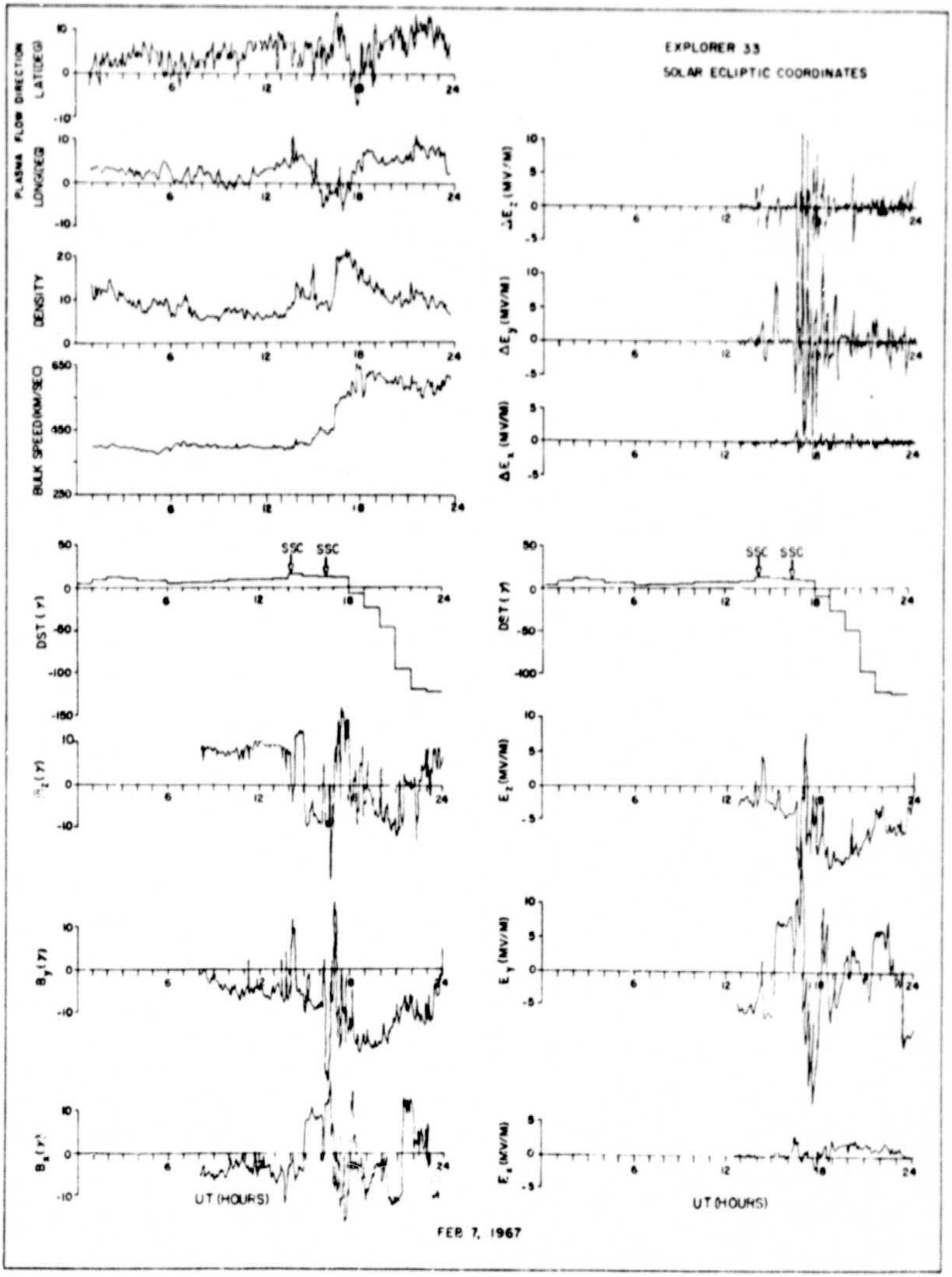
EXPLORER 33
SOLAR ECLIPTIC COORDINATES
PLASMA FLOW DIRECTION
LAT(DEG)
LONG(DEG)
DENSITY
BULK SPEED(KM/SEC)
DST (γ)
SSC
SSC
B_z(γ)
B_y(γ)
B_x(γ)
ΔE_z (MV/M)
ΔE_y (MV/M)
ΔE_x (MV/M)
E_z (MV/M)
E_y (MV/M)
E_x (MV/M)
UT (HOURS)
UT (HOURS)
FEB 7, 1967

Figure 1

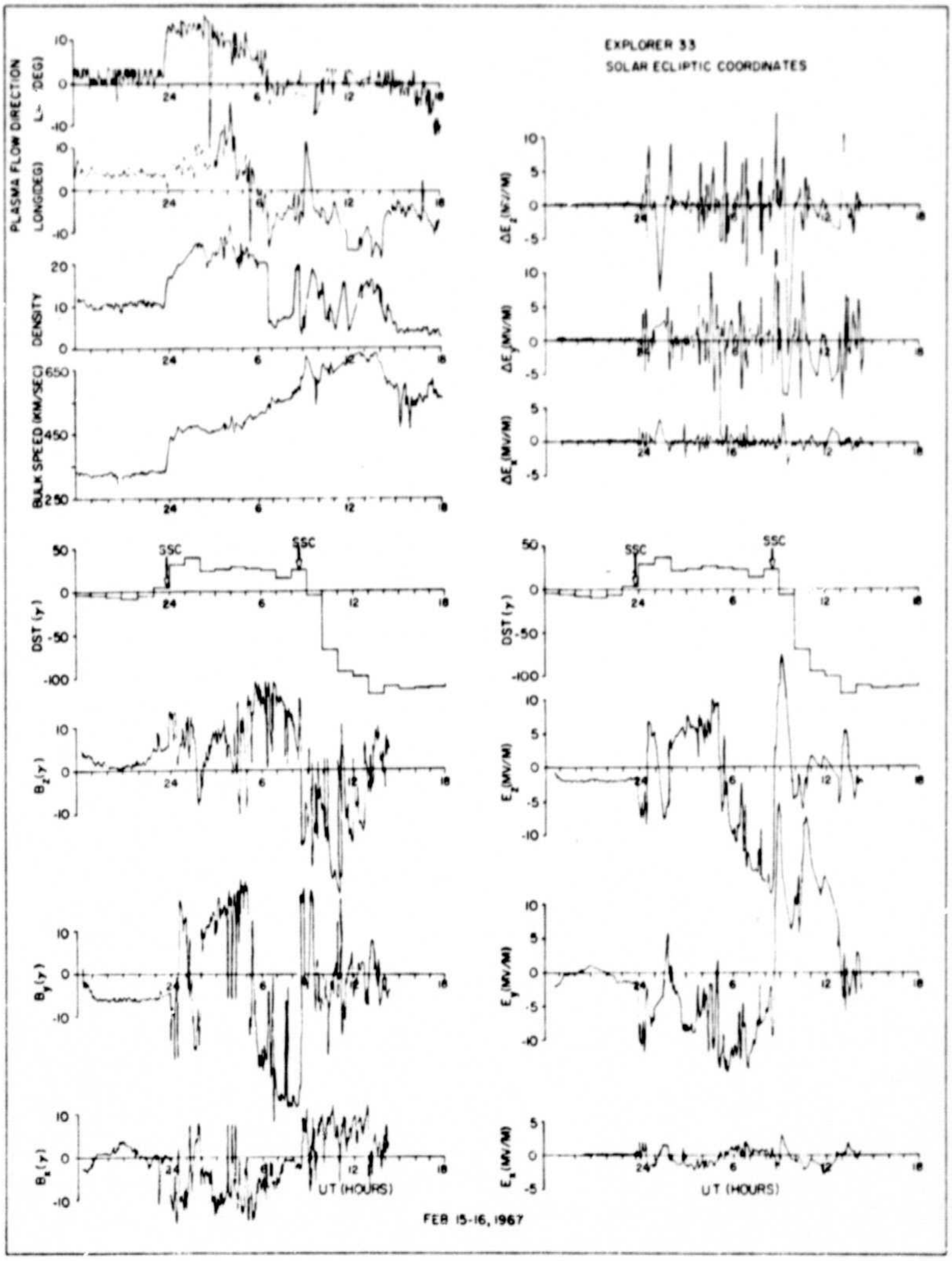
EXPLORER 33
SOLAR ECLIPTIC COORDINATES
PLASMA FLOW DIRECTION
DENSITY
BULK SPEED (KM/SEC)
DST (γ)
SSC
UT (HOURS)
FEB 15-16, 1967

Figure 2

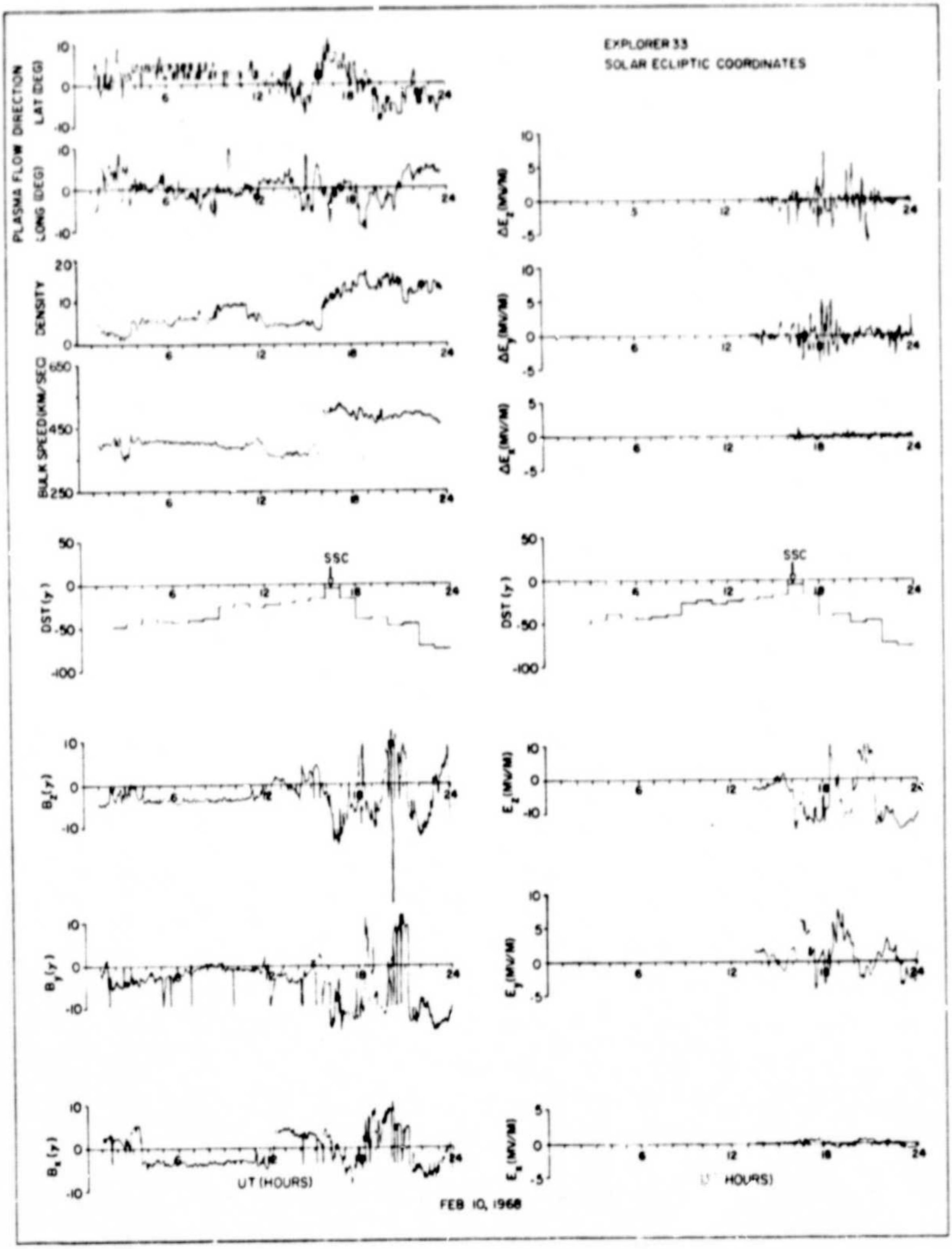
EXPLORER 33
SOLAR ECLIPTIC COORDINATES
PLASMA FLOW DIRECTION
LAT (DEG)
LONG (DEG)
DENSITY
BULK SPEED (KM/SEC)
DST (γ)
SSC
B_z (γ)
B_y (γ)
B_x (γ)
ΔE_z (MV/M)
ΔE_y (MV/M)
ΔE_x (MV/M)
E_z (MV/M)
E_y (MV/M)
E_x (MV/M)
UT (HOURS)
FEB 10, 1968

Figure 3

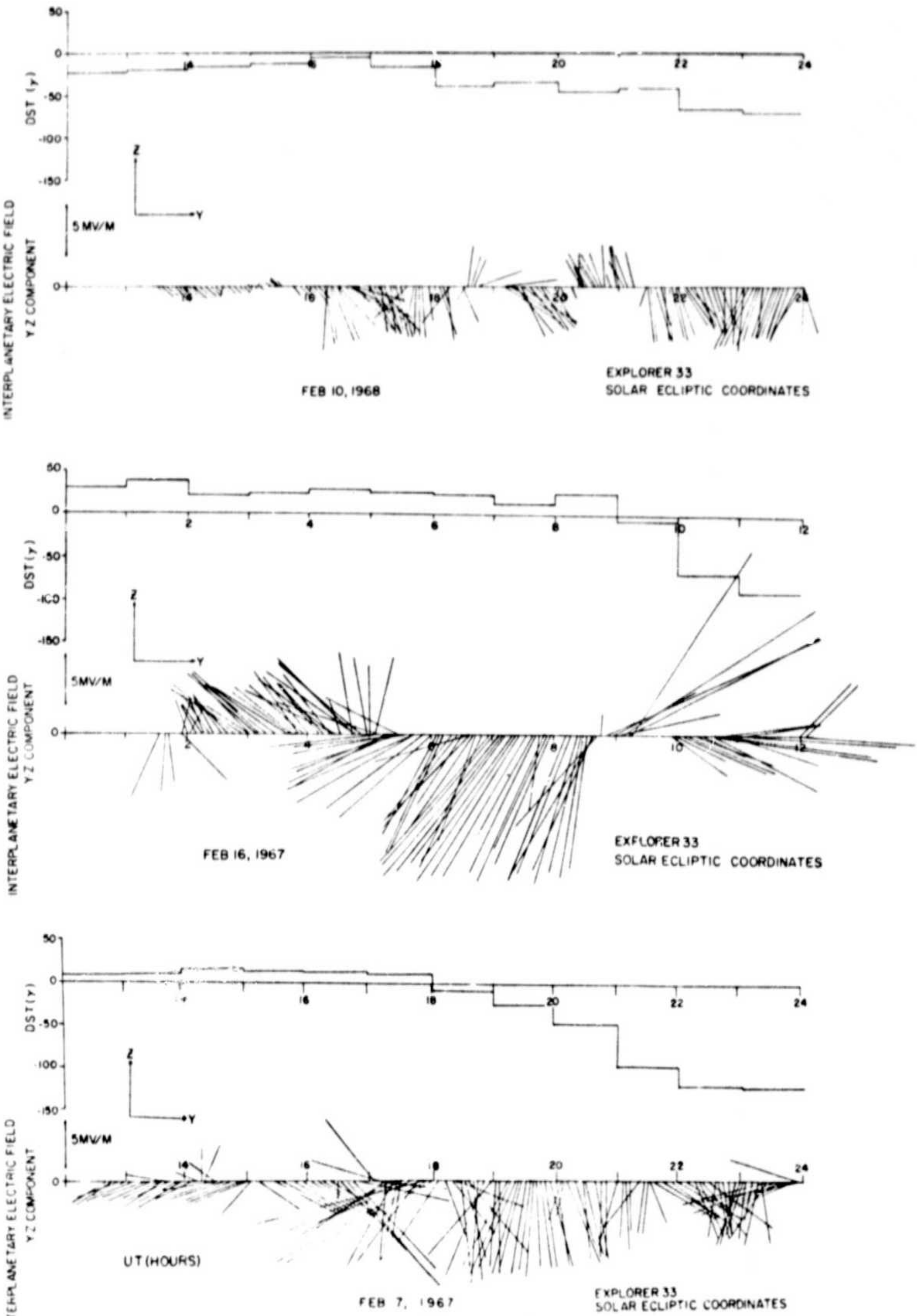
DST (γ)
INTERPLANETARY ELECTRIC FIELD
Y Z COMPONENT
5 MV/M
FEB 10, 1968
EXPLORER 33
SOLAR ECLIPTIC COORDINATES
FEB 16, 1967
EXPLORER 33
SOLAR ECLIPTIC COORDINATES
UT (HOURS)
FEB 7, 1967
EXPLORER 33
SOLAR ECLIPTIC COORDINATES

Figure 4

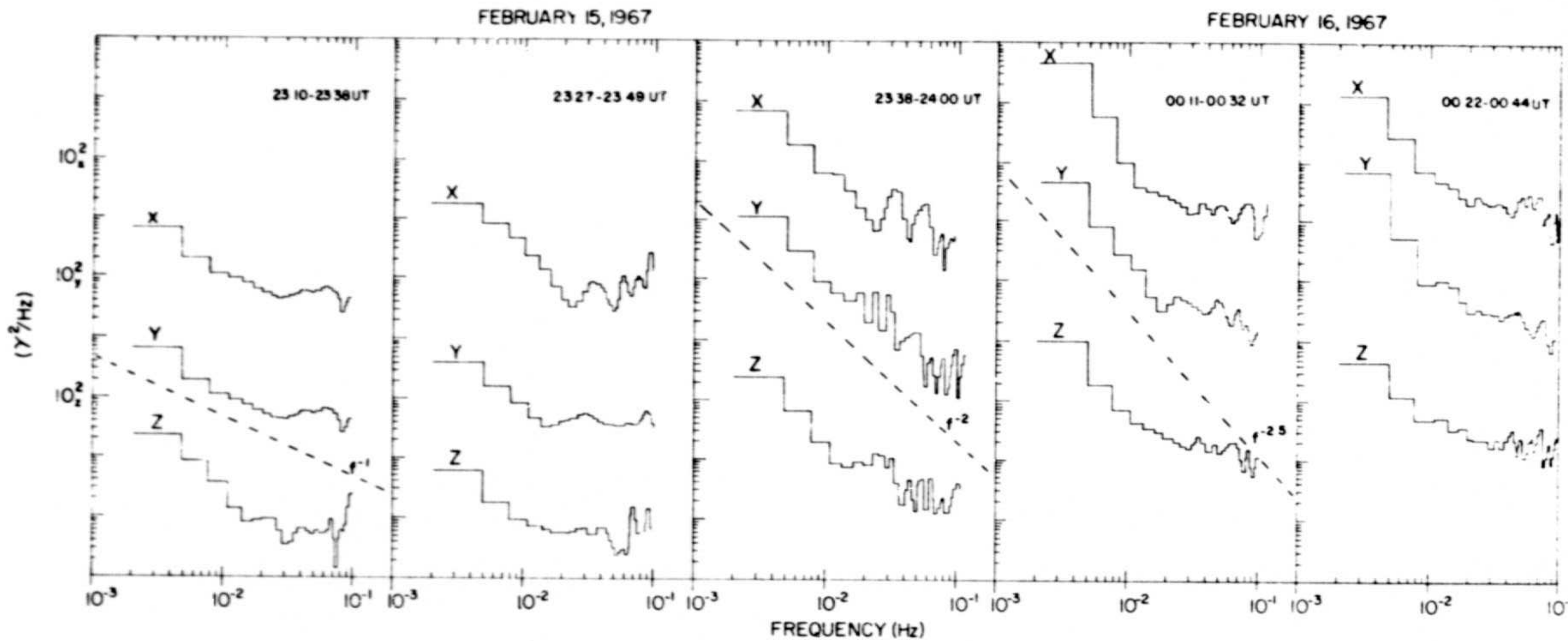
FEBRUARY 15, 1967
FEBRUARY 16, 1967
23 10-23 38 UT
23 27-23 49 UT
23 38-24 00 UT
00 11-00 32 UT
00 22-00 44 UT
X
Y
Z
FREQUENCY (Hz)

Figure 5

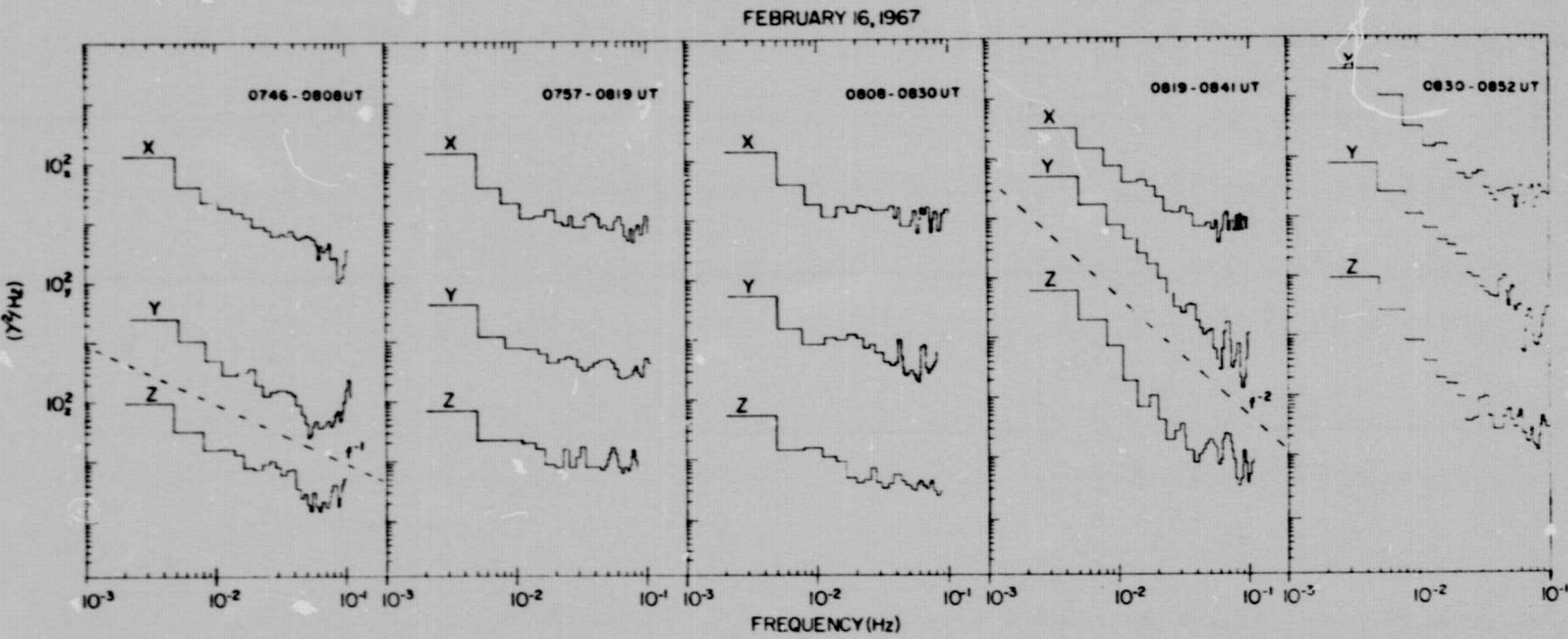
FEBRUARY 16, 1967
0746-0808UT
0757-0819 UT
0808-0830 UT
0819-0841 UT
0830-0852 UT
X
Y
Z
f^{-1}
f^{-2}
(γ^2/Hz)
10^2_x
10^2_y
10^2_z
10^{-3}
10^{-2}
10^{-1}
FREQUENCY (Hz)

Figure 6

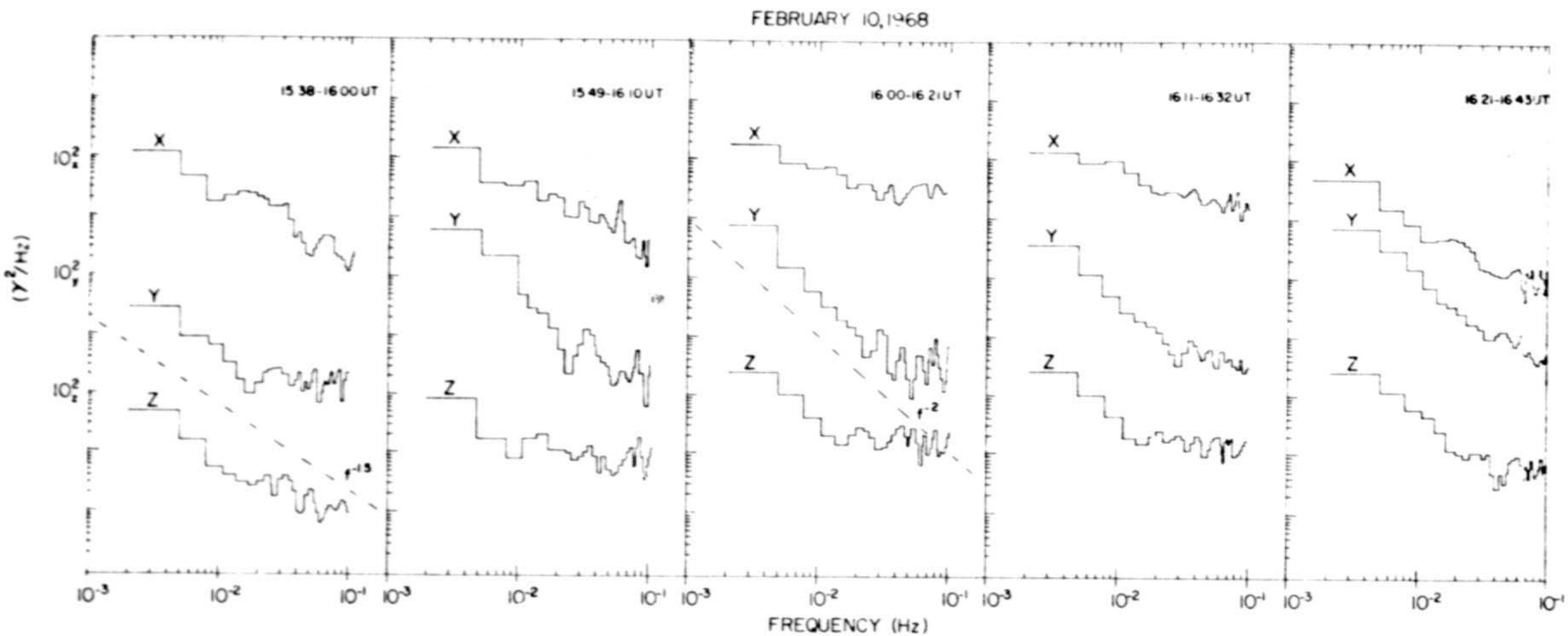

FEBRUARY 10, 1968
15 38-16 00 UT
15 49-16 10 UT
16 00-16 21 UT
16 11-16 32 UT
16 21-16 43 UT
X
Y
Z
$f^{-1.5}$
f^{-2}
(γ^2/Hz)
10^{-3}
10^{-2}
10^{-1}
FREQUENCY (Hz)

Figure 7